Monte Carlo simulation-based simulation of shadow occlusion efficiency of a heliostat field

Tao Qin [1, *, #], Tianyu Hou [2, #], Yixin Lin [1, #]

[1] School of Statistics and Mathematics, Shandong University of Finance and Economics, Jinan, China, 250014

[2] School of Management Science and Engineering, Shandong University of Finance and Economics, Jinan, China, 250014

* Corresponding author: 13259599628@163.com

[#]These authors contributed equally.

Abstract. Tower solar photovoltaic power plant has a broad application prospect as a sustainable energy solution, in which the shadow occlusion efficiency, as an important part of the optical efficiency of the mirror field, has always been a computational difficulty. In this paper, the geometric projection method and Monte Carlo algorithm are used to explore the shadow occlusion efficiency of a heliostat field, and the two parts of shadowing and occlusion are simulated based on the coordinate transformation under the mirror field coordinate system. By calculating the shadow occlusion efficiency, the energy loss of the heliostat system can be evaluated, and then the system design can be optimized to improve the energy harvesting efficiency of the system.

Keywords: Heliostat Field, Geometric Projection, Monte Carlo, Shadow Occlusion Efficiency.

1. Introduction

In the tower solar power generation system, the role of the heliostat is to reflect the radiated sunlight effectively to the collector at the top of the absorber tower for subsequent subsystems, which is the key part of the whole power plant [1]. Among them, the shadow occlusion efficiency of the heliostat field has always been a research difficulty, for this problem, scholars in various countries have proposed many computational methods: DELSOL [2], CFD [3], SCT [4], etc, which were highly favored in the early stage of the research, but all of them have certain shortcomings, such as slow computation speed, inability to good In order to simulate the mirror field shadow occlusion, for this defect, this paper chooses to combine the geometric projection method and Monte Carlo simulation, which are applied in different stages of simulation, respectively, to better simulate the process of mirror field shadow occlusion in the fixed-sun field, and improve the computational efficiency, which is of great significance for the operation and maintenance of the solar power generation system.

2. Modelling

2.1. Mirror field design parameters and modeling assumptions

In order to facilitate the reading of data, this paper selects the site observation data located in the east longitude, north latitude altitude 3000 meters, the specific parameters are shown in Table 1.

Table 1. Mirror field design parameters

form	variant	parameter
field of mirrors	Mirror field shape	Circular with a radius of 350m
	distance between the centers of adjacent heliostats	$\leqslant 5m$
Tropic of Cancer	Sunset Mirror Size	$6m \times 6m$
	Mounting Height	$4m$
	Total number of heliographs	1745
heaters	high degree	8m
	calibre	7m

The layout of the heliostat field of the tower solar power system is shown in the table above, and some basic assumptions in the modeling process are as follows:

(1) It is assumed that the mirror surface of the heliostat mirror is a continuous plane and there is no unevenness on the mirror surface;

(2) The solar beam incident on the mirror surface is approximated as a 9. 3 mrad solar cone.

2.2. Shadow Occlusion Efficiency

The shadow occlusion of a heliostat consists of two parts, the shadow efficiency and the occlusion efficiency, and the shadow occlusion usually occurs between two and more heliostats [5]. As shown in Figure 1, part of the mirror of heliostat 1 is in the shadow of heliostat 2 and cannot reflect sunlight efficiently, resulting in energy loss called occlusion loss, and part of the sunlight reflected by heliostat 1 is blocked by heliostat 3, and cannot be propagated to the collector resulting in loss called occlusion loss. The physical significance of the shadow occlusion efficiency for the mirror field can reflect sunlight to the collector without being blocked by the sum of the mirror area and the ratio of the total mirror area installed in the mirror field.

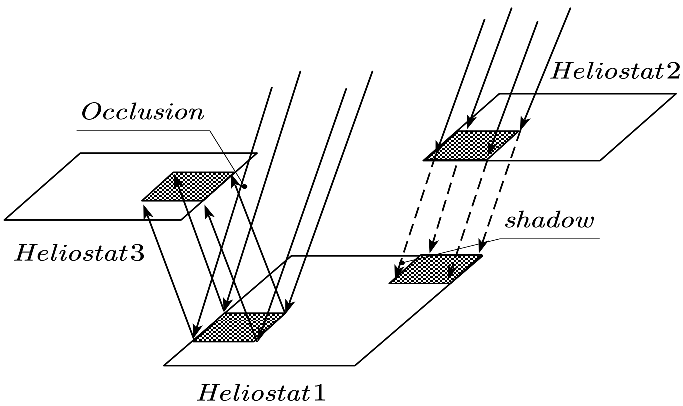

Figure 1. Schematic illustration of the occlusion and occlusion efficiencies of heliostats

2.2.1. Geometric projection method to determine the shadow and occlusion of the heliostat

For any heliostat, its convergence of sunlight will inevitably reflect convergence on the collector at a point, according to reference [6], the unit reflection vector of a ray of light from the center of the mirror of a heliostat pointing toward the center of the collector can be expressed as:

$$S_{i,j} = \frac{O - O_i}{|O - O_i|} = \frac{(-x_i, -y_i, H_j - Z_i)}{\sqrt{x_i^2 + y_i^2 + (H_j - Z_i)^2}} \tag{1}$$

The unit vector of the incident light is denoted as $S_{i,s} = (x_i, y_i, z_i)$, $S_{i,s}$ in the mirror field coordinate system:

$$\begin{cases} x_i = \cos(a_s)\cos(\gamma_s - \frac{\pi}{2}) \\ y_i = \cos(a_s)\sin(\gamma_s - \frac{\pi}{2}) \\ z_i = \sin(a_s) \end{cases} \tag{2}$$

Where α_s and γ_s are the solar altitude angle and azimuth angle, respectively, which are obtained from reference [7] and are calculated as follows:

$$\sin\alpha_s = \cos\delta\cos\varphi\cos\omega + \sin\delta\sin\varphi \tag{3}$$

$$\cos\gamma_s = \frac{\sin\delta - \sin\alpha_s\sin\varphi}{\cos\alpha_s\cos\varphi} \tag{4}$$

Where φ is the local latitude, δ is the solar declination angle, and ω is the solar time angle, which can be derived from the following equations, respectively [8]:

$$\delta = \frac{23.45\pi}{180}\sin\frac{2\pi D}{365} \tag{5}$$

$$\omega = \frac{\pi}{12}(T - 12) \tag{6}$$

Where D is the number of days counted from the vernal equinox as day 0, T is the local time, for the time of a whole point, it is directly brought to a whole number, and for the time of a half-point, the 30 minutes are counted as 0.5 instead. Then the unit mirror normal vector of the heliostat is expressed as:

$$k_f = \frac{S_{i,s} - S_{i,\ j}}{|S_{i,s} - S_{i,\ j}|} \tag{7}$$

There are three kinds of tracking methods for heliostat visual sun track, single-axis tracking, dual-axis tracking and polar-axis tracking, and in practice, most heliostats use dual-axis tracking methods [9]. In this paper, the azimuth-height angle biaxial tracking method is used to determine the vertex coordinates of the heliostat by means of coordinate rotation. The rotation in the XOZ plane is shown in Figure 2 and the rotation in the XOY plane is shown in Figure 3.

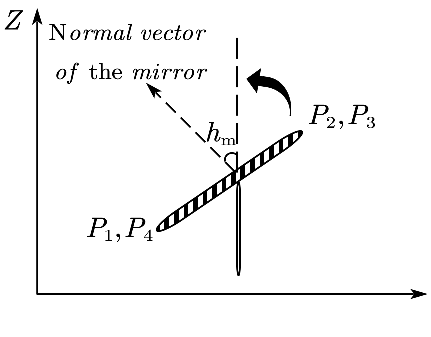

Figure 2. Rotation along the XOZ plane

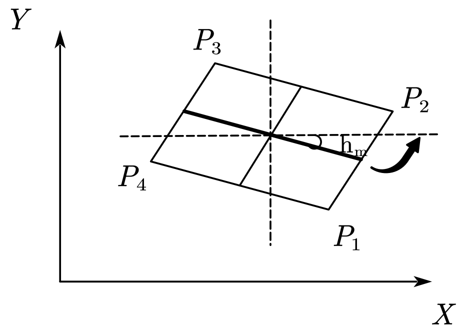

Figure 3. Rotation along the XOY plane

The rotation matrix of the fixed heliograph is $R = R_x \times R_y$. The rotation process of the point P_i is:

$$P_r = R \cdot P_i = \begin{bmatrix} \cos(-p_m) & -\cos(h_m)\cdot\sin(-p_m) & \sin(-p_m)\cdot\sin(h_m) \\ \sin(-p_m) & -\cos(p_m)\cdot\cos(h_m) & -\cos(-p_m)\cdot\sin(h_m) \\ 0 & \sin(h_m) & \cos(h_m) \end{bmatrix} \cdot P_z \tag{8}$$

Where p_m and h_m are the heliostat altitude and azimuth angles, respectively, which are calculated as follows according to the literature [10]:

$$h_m = \arcsin\sqrt{1-k_f^2} \tag{9}$$

$$p_m = -\arccos\frac{k_y}{\sqrt{k_x^2+k_y^2}} \tag{10}$$

In the first quadrant, the coordinates of rotation of the vertices of a heliostat with (x_0, y_0, z_0) as the center of the mirror are:

$$P_1 = \begin{cases} x_0 + \frac{1}{2}L_1\cdot\frac{k_y}{\sqrt{k_x^2+k_y^2}} + \frac{1}{2}L_2\cdot\frac{k_y}{\sqrt{k_x^2+k_y^2}}\cdot k_z \\ y_0 + \frac{1}{2}L_1\cdot\frac{k_x}{\sqrt{k_x^2+k_y^2}} - \frac{1}{2}L_2\cdot\frac{k_x}{\sqrt{k_x^2+k_y^2}}\cdot k_z \\ z_0 - \frac{1}{2}L_2\cdot\sqrt{1-k_z^2} \end{cases} \quad P_2 = \begin{cases} x_0 + \frac{1}{2}L_1\cdot\frac{k_y}{\sqrt{k_x^2+k_y^2}} - \frac{1}{2}L_2\cdot\frac{k_x}{\sqrt{k_x^2+k_y^2}}\cdot k_z \\ y_0 + \frac{1}{2}L_1\cdot\frac{k_x}{\sqrt{k_x^2+k_y^2}} + \frac{1}{2}L_2\cdot\frac{k_x}{\sqrt{k_x^2+k_y^2}}\cdot k_z \\ z_0 + \frac{1}{2}L_1\cdot\sqrt{1-k_z^2} \end{cases}$$

$$P_3 = \begin{cases} x_0 - \frac{1}{2}L_1\cdot\frac{k_y}{\sqrt{k_x^2+k_y^2}} - \frac{1}{2}L_2\cdot\frac{k_x}{\sqrt{k_x^2+k_y^2}}\cdot k_z \\ y_0 - \frac{1}{2}L_1\cdot\frac{k_x}{\sqrt{k_x^2+k_y^2}} + \frac{1}{2}L_2\cdot\frac{k_x}{\sqrt{k_x^2+k_y^2}}\cdot k_z \\ z_0 + \frac{1}{2}L_2\cdot\sqrt{1-k_z^2} \end{cases} \quad P_4 = \begin{cases} x_0 - \frac{1}{2}L_1\cdot\frac{k_y}{\sqrt{k_x^2+k_y^2}} + \frac{1}{2}L_2\cdot\frac{k_x}{\sqrt{k_x^2+k_y^2}}\cdot k_z \\ y_0 - \frac{1}{2}L_1\cdot\frac{k_x}{\sqrt{k_x^2+k_y^2}} - \frac{1}{2}L_2\cdot\frac{k_x}{\sqrt{k_x^2+k_y^2}}\cdot k_z \\ z_0 - \frac{1}{2}L_2\cdot\sqrt{1-k_z^2} \end{cases} \tag{11}$$

For the transformation of the coordinates of points on a fixed heliograph that are in quadrants two, three, and four, the calculation is the same as above.

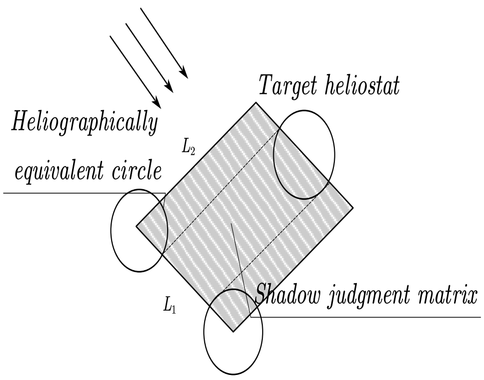

Figure 4. Shadow judgment rectangle top view

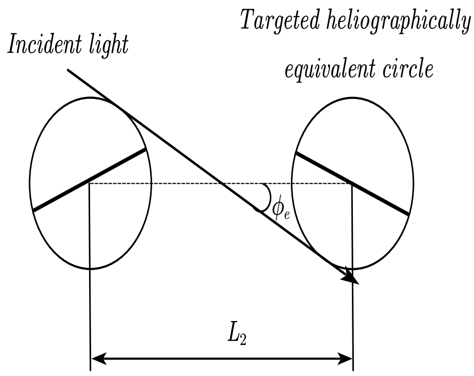

Figure 5. Shadow judge rectangular side view

Based on the physical significance of shadow occlusion, the heliostat that causes shadow occlusion can be determined by the shadow occlusion judgment rectangle. If the center point of a heliostat lies within the shadow occlusion judgment rectangle, it will cause shadow occlusion to the target heliostat. As shown in Figures 4 and 5, the formula for calculating the two sets of side lengths L_1, L_2 of the occlusion judgment rectangle is:

$$\begin{cases} L_1 = 2l_m \\ L_2 = w_m/\sin\phi_e \end{cases} \tag{12}$$

Where l_m, w_m is the length and width of the heliostat, respectively, further yielding the coordinates of the four fixed points $d_1 \sim d_4$ of the shaded rectangle:

$$d_1\!:\!\begin{cases} x_{d1} = x_i + L_1 \cdot v_y \\ y_{d1} = y_i + L_1 \cdot v_x \end{cases} \qquad d_2\!:\!\begin{cases} x_{d2} = x_i + L_1 \cdot v_y \\ y_{d2} = y_i - L_1 \cdot v_x \end{cases}$$
$$d_3\!:\!\begin{cases} x_{d3} = x_i + L_1 \cdot v_y + L_2 \cdot v_x \\ y_{d3} = y_i + L_1 \cdot v_x + L_2 \cdot v_y \end{cases} \qquad d_4\!:\!\begin{cases} x_{d4} = x_i - L_1 \cdot v_y + L_2 \cdot v_x \\ y_{d4} = y_i + L_1 \cdot v_x + L_2 \cdot v_y \end{cases} \tag{13}$$

Where (x_i, y_i, z_i) is the center coordinate of the target heliostat mirror, and u_x, u_y is calculated by the formula:

$$\mu_x = \frac{x_i}{\sqrt{x_i^2 + y_i^2}} \tag{14}$$

$$\mu_y = \frac{y_i}{\sqrt{x_i^2 + y_i^2}} \tag{15}$$

According to the center coordinates of the heliostat mirror and the positions of the four fixed point coordinates of the occlusion judgment rectangle, it can be determined whether the center of the heliostat mirror is located in the occlusion rectangle, so as to determine whether the heliostat is occlusion the target heliostat. Similarly, by replacing the incident light with the reflected light, it can be determined whether the center of the heliostat mirror is located in the occlusion rectangle, thus determining whether the heliostat causes occlusion to the target heliostat.

2.2.2. Monte Carlo simulation algorithm to calculate the shadow obscuration efficiency of the mirror field

In order to accurately calculate the shadow obscuration part on the target heliostat mirror, this paper uses the Monte Carlo algorithm to solve for the shadow obscuration efficiency.

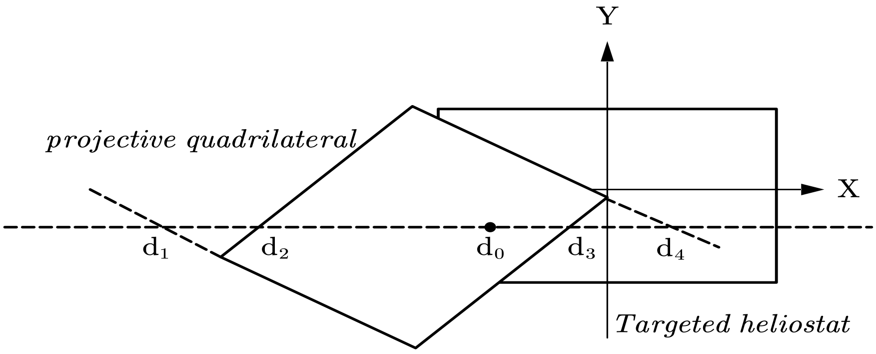

Figure 6. Schematic for determining whether a random point is obscured by a shadow

As shown in Figure 6, d_0 is a random point on the mirror surface of the target heliostat, over this point d_0 as a straight line parallel to the X-axis or Y-axis of the coordinate system of the target heliostat, the intersection of the straight line with the opposite side of the projected quadrilateral or the extension line is recorded as $d_1 \sim d_4$, which corresponds to the X-axis coordinates of $x_{d_1} \sim x_{d_4}$ [11]. When the random point d_0 lies within the projection quadrilateral, $x_{d_1} \sim x_{d_4}$ and x_{d_0} satisfy the relation:

$$\begin{cases}(x_{d1}-x_{d0})(x_{d3}-x_{d0})<0\\(x_{d2}-x_{d0})(x_{d4}-x_{d0})<0\end{cases}\tag{16}$$

It means that the random point d_0 is shaded, otherwise it means that the random point d_0 is not shaded. Let the number of random points obscured by shadows be N_{shield}, and the total number of randomly generated points in a large number scattered uniformly on the mirror of the target heliostat be N_{total}, then the shadow obscuring efficiency η_{sb} of the target heliostat is:

$$\eta_{sb}=1-\frac{\eta_{shield}}{N_{total}}\tag{17}$$

The specific Monte Carlo algorithmic procedure is as follows:

Step1: Generate random incident light vectors

Select an untreated heliostat as the target heliostat, and generate random incident light vectors in the range of tangential angle not exceeding rad.

Step2: Generate random reflected light vector

Combine the random incident light vector generated in Step1 and the normal vector of the mirror surface at the point to generate the random reflected light vector.

Step3: Calculate the rotation matrix

Calculate the rotation matrix from the mirror field coordinate system to the mirror coordinate system to determine the coordinates of each vertex of a single mirror.

Step4: Determine the shadow occlusion

Sprinkle random points on the mirror surface of the target heliostat, and judge the positional relationship between the random points on the mirror surface and the projection quadrilateral formed by the heliostat that causes shadow occlusion, so as to determine the random mirror points that are not occluded by shadows.

Step5: Calculate the shadow occlusion efficiency

Repeat the above Step1- Step4 operation 10000 times to calculate the shadow occlusion efficiency η_{sb}.

After several simulations, the annual variation of the shadow occlusion efficiency for the average month in a year is obtained as shown in Table 2, from which it can be seen that the shadow occlusion efficiency shows an increasing and then decreasing trend in a year.

Table 2. Annual variation of shadow occlusion efficiency

Month	1	2	3	4	5	6
η_{sb}	0. 8978	0. 9165	0. 9237	0. 9226	0. 9221	0. 9219
Month	7	8	9	10	11	12
η_{sb}	0. 9221	0. 9227	0. 9226	0. 9147	0. 8976	0. 8865

3. Conclusion

In this study, the geometric projection method and Monte Carlo algorithm were applied to simulate the tower solar heliostat field by exploring the shadow occlusion efficiency, and the trend of annual shadow occlusion efficiency was obtained. The data analysis reveals the difference in energy loss in different months, which provides a basis for system performance evaluation. For the optimized design, adjusting the mirror arrangement or increasing the number of collectors for months with high shadow occlusion efficiency can effectively reduce the energy loss. Meanwhile, the knowledge of system performance in different seasons helps to develop seasonal adjustment strategies to improve system reliability and stability.

Despite the results achieved in this study, there is still much room for improvement in integrating with practice. First, the stochastic nature of Monte Carlo simulation may lead to differences in the results, and multiple calculations are needed to improve reliability. Second, some of the influencing factors were simplified in the modeling process, and more environmental factors can be considered; this study assumed that the heliostat is planar, and assumed that the weather is sunny, and did not take into account the concentration of light under cloudy and overcast conditions, and subsequent studies need to consider the above factors. Therefore, future research will be devoted to improving the simulation accuracy, considering more factors on the shadow occlusion efficiency, and exploring more reliable algorithms to optimize the performance of solar heliostat fields to provide more reliable solutions for the renewable energy field.

References

[1] H. Li. Modeling and simulation research on tower solar thermal power generation heat transfer and energy storage system [D]. North China Electric Power University, 2019.

[2] Sun H. Research and optimization of heliostat field layout based on mixed-strategy whale optimization algorithm [D]. Lanzhou Jiaotong University, 2022.

[3] W. J. Lou, H. Y. Shan, Z. Yang, H. W. Xu. Study on the occlusion effect of the body shape coefficient of ultra-large array photovoltaic panels [J]. Journal of Building Structures, 2021, 42 (05): 47 - 54.

[4] Sánchez M, Romero M. Methodology for generation of heliostat field layout incentral receiver systems based on yearly normalized energy surfaces [J]. Solar Energy, 2006, 80 (7): 861 - 874.

[5] J. W. Wang. Design of heliostat tracking control system for tower solar thermal power plant [J]. Shanghai Electric Technology, 2019, 12 (03).

[6] Liu Jianxing. Optical efficiency modeling simulation and optimal arrangement of heliostat field for tower-type photovoltaic power plant[D]. Lanzhou Jiaotong University, 2022.

[7] Dong Dengguo. Research on solar tracking control system[D]. North University of China, 2023.

[8] Solar Declination [1] Ding Yan, Yuan Longji, Zhao Peitao et al. Research on the tracking algorithm of solar apparent sun trajectory [J]. Energy Conservation, 2020, 39 (11).

[9] WANG Xinyu, LI Lan, GUO Minghuan, WANG Zhifeng, LI Xigang, ZHANG Xiliang. Tracking practice of azimuth-pitch biaxial tracking heliostat [J]. Journal of Solar Energy, 2020, 41 (11): 212 - 219.

[10] Height angle of heliostat [1] J. Y. Liu. Design of tower solar heliostat tracking control system [D]. North Central University, 2022.

[11] X. Zhao. Optimization of mirror field scheduling for tower solar thermoelectric system [D]. Zhejiang University, 2017.